Oncogenic K-Ras Regulates Proliferation and Cell Junctions in Lung Epithelial Cells through Induction of Cyclooxygenase-2 and Activation of Metalloproteinase-9

Xue-Qing Wang,* Howard Li,* Vicki Van Putten,* Robert A. Winn,*
Lynn E. Heasley,[†] and Raphael A. Nemenoff*

Departments of *Medicine and [†]Craniofacial Biology, University of Colorado Denver, Denver, CO 80262

Expression of oncogenic K-Ras is frequently observed in non–small-cell lung cancer. However, oncogenic K-Ras is not sufficient to transform lung epithelial cells and requires collaborating signals that have not been defined. To examine the biological effects of K-Ras in nontransformed lung epithelial cells, stable transfectants were generated in RL-65 cells, a spontaneously immortalized lung epithelial cell line. Expression of K-Ras resulted in extracellular signal-regulated kinase (ERK) activation, which mediated induction of cyclooxygenase (COX)-2 and increased prostaglandin E_2 production. Epithelial cells expressing oncogenic K-Ras showed increased proliferation in two- and three-dimensional tissue culture and delayed formation of hollow acinar structures in three-dimensional matrigel cultures. These affects were mediated through COX-2–dependent activation of β-catenin signaling and inhibition of apoptosis. ERK activation also led to induction of metalloproteinase (MMP)-9 and cleavage of E-cadherin at two specific sites. This resulted in partial disruption of adherens junctions as determined by decreased transepithelial resistance (TER), and disruption of E-cadherin/β-catenin interactions. An MMP-9 inhibitor reversed the decrease in TER and inhibited β-catenin signaling. These data indicate that although expression of oncogenic K-Ras does not transform lung epithelial cells, it alters the phenotype of the cells by increasing proliferation and decreasing cell–cell contacts characteristic of epithelial cells.

INTRODUCTION

Activating mutations in Ras proteins are common in many types of cancer. In non–small-cell lung cancer (NSCLC), the incidence of activating mutations in K-Ras is between 30 and 50%. Similarly, in chemically induced lung tumors in mice, activating mutations in K-Ras are observed early on after administration of carcinogen (Horio *et al.*, 1996). Mouse models have been developed in which activation of K-Ras is sufficient to induce lung tumor formation (Johnson *et al.*, 2001). However, in cultured lung epithelial cells, expression of gain-of-function K-Ras is not sufficient to induce transformation, as assessed by colony formation in soft agar or tumor formation in xenografts (Sato *et al.*, 2006). Although it is presumed that additional signaling pathways collaborate with K-Ras, leading to transformation, these pathways have not been identified. Activation of Ras leads to stimulation of the Raf/mitogen-activated protein kinase kinase (MEK)/extracellular signal-regulated kinase (ERK) pathway, as well as the activation of phosphatidylinositol 3-kinase (PI3-kinase), resulting in Akt activation (Campbell *et al.*, 1998). Gain-of-function forms of K-Ras also lead to induction of cyclooxygenase (COX)-2 expression, with commensurate in-creases in prostaglandin (PG) E_2 production (Sheng *et al.*, 1998; Blaine *et al.*, 2001). In fact, NSCLC cell lines expressing oncogenic K-Ras have constitutively high levels of COX-2 and PGE_2 production, which is required for transformed growth of these cells (Heasley *et al.*, 1997; Dannenberg *et al.*, 2001). However, mechanisms whereby PGE_2 promotes cancer growth and progression are not well understood.

Epithelial-mesenchymal transition (EMT) is a complex process during which epithelial cells lose cell–cell interactions, leading to loss of polarity and disruption of tight junctions (for review, see Huber *et al.*, 2005). This is associated with alterations in the polarized distribution of cytoskeleton components, resulting in increased motility and invasiveness. EMT participates in several morphogenetic processes during embryonic development and has been proposed to play a key role in cancer metastasis. The process of EMT includes two distinct steps: the disruption of intercellular junctions associated with decreased levels of epithelial markers, and increased expression of mesenchymal markers. Disruption of intercellular junctions may involve transcriptional repression of cell–cell adhesion proteins. However, recent studies have shown that posttranslational modification of these proteins plays an important role in controlling epithelial phenotype.

Cadherins are a family of Ca^{2+}-dependent transmembrane glycoproteins that mediate cell–cell adhesion through forming homophilic interactions in a zipper-like manner, and they play essential roles in cell polarity by inducing cytoskeleton protein rearrangement (Pokutta and Weis, 2007). E-cadherin, the prototypic member of cadherin family, mediates homotypic cell adhesion in epithelia. Intercellular interactions between E-cadherin proteins on adjacent

cells result in strong cell–cell adhesion, and they are critical for establishment of epithelial cell polarity. The cytoplasmic domain of E-cadherin binds to α- and β-catenin, linking adherens junctions to the actin cytoskeleton (Halbleib and Nelson, 2006). Down-regulation of E-cadherin expression can lead to loss of cell adhesions, increased proliferation, and tumor invasiveness as seen in many epithelially derived tumors (Thiery, 2002). The expression and function of E-cadherin is regulated by intracellular signals and surrounding environment. For example, overexpression of Bcl-2 in both MCF-7 and Madin-Darby canine kidney epithelial cells decreased levels of functional E-cadherin, thereby interfering with junction formation, which resulted in the loss of contact inhibition (Li *et al*., 2003). Cell adhesion molecule L1 expression in MCF-7 cells leads to the disruption of adherens junctions and increased β-catenin transcriptional activity (Shtutman *et al*., 2006). Collagen type I induces disruption of E-cadherin–mediated cell–cell contacts and promotes proliferation of pancreatic carcinoma cells (Koenig *et al*., 2006). Thus, the ability of E-cadherin to mediate cell–cell contact had been suggested to be a major factor influencing cell contact growth inhibition. Other examples of adhesion loss include E-cadherin extracellular domain mutants (Sasaki *et al*., 2000) or disruption of the link to actin through catenins (Perez-Moreno and Fuchs, 2006). In all the cases, alterations in adherens junctions initiates cascades of signals that result in cytoskeleton reorganization, cross-talking to intracellular signals, and eventually to gene transcription.

The Ras pathway has also been implicated in the cytoskeleton rearrangement and cell migration that accompany cell dispersion through PI3 kinase (Potempa and Ridley, 1998).
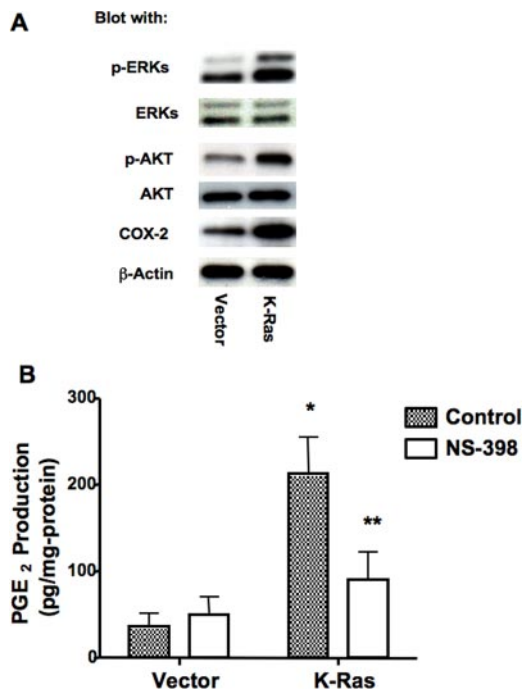

Figure 1. Expression of oncogenic K-Ras induced COX-2 and PGE$_2$ production. (A) Cell lysates were prepared from RL-65 cells stably transfected with empty vector (vector) or oncogenic K-Ras and immunoblotted for the indicated proteins. (B) Empty vector controls or K-Ras cells were pretreated for 48 h with 10 μM NS-398 or vehicle (dimethyl sulfoxide [DMSO]). Release of PGE$_2$ into the BPE-free media for 2 h, PGE$_2$ level was determined by ELISA as described in *Materials and Methods*. *p $<$ 0.05 versus vector; **p $<$ 0.05 versus control.
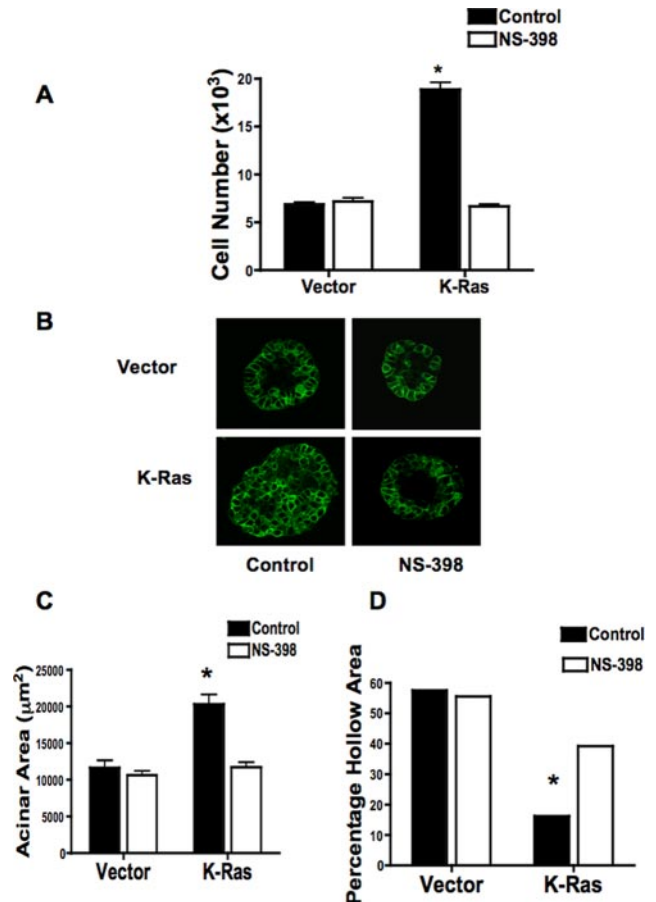

Figure 2. Effects of K-Ras on Growth of RL-65 Cells in two- and three-dimensional tissue culture are reversed by COX-2 Inhibition. (A) The indicated cells were plated in media lacking BPE in the presence of 20 μM NS-398 or vehicle (0.1% DMSO), and grown for 72 h. Cell number was determined as described in *Materials and Methods*. *p $<$ 0.05 versus vector control. (B) Cells were plated in three-dimensional Matrigel culture as described in *Materials and Methods*. After 5 d in culture, structures were fixed and stained for E-cadherin (green). Representative acinar structures are shown. (C and D) Acinar structures obtained in B were quantitated. Size of individual acini in diameter was determined at 5 d (C). The percentage of the hollow area was calculated by dividing the hollow area by the total area for each structure (D). At least 20 acini were analyzed for each experiment, and results represent the mean of two independent experiments with the SEM indicated. *p $<$ 0.05 versus vector control.

The Raf/mitogen-activated protein kinase (MAPK) pathway promotes the migration of fibroblastic cells and is necessary for Ras induced transformation of NIH 3T3 cells (Bollag *et al*., 1996). The MAPK pathway is also known to affect the actin–myosin system and leads to increased migration of COS-7 cells (Potempa and Ridley, 1998). To develop a better understanding of the biological effects of oncogenic K-Ras on nontransformed lung epithelial cells, we have developed stable transfectants of RL-65 cells, a spontaneously immortalized rat lung epithelial cell line expressing gain-of-function K-Ras. In this study, we examined the effects of K-Ras on proliferation and alterations in cell–cell contacts. Our data indicate that induction of COX-2 and metalloproteinase (MMP)-9 cooperate to increase β-catenin signaling, stimulate proliferation, and alter adherens junctions.
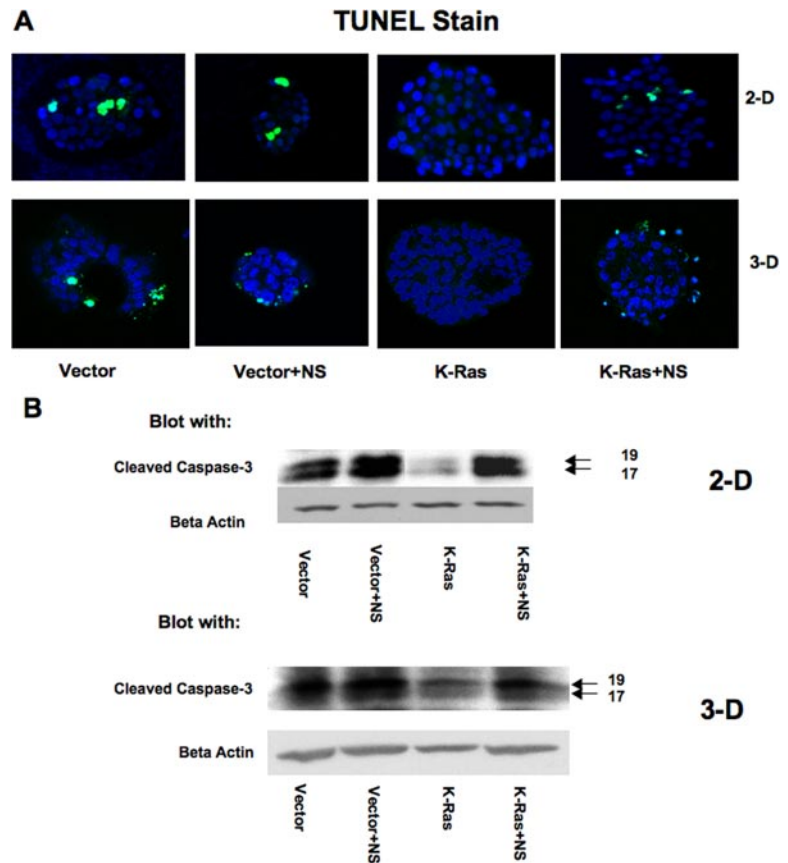
Figure 3. Expression of K-Ras on apoptosis are reversed by COX-2 inhibition. (A) The indicated cells were grown for 3 d in 2D culture or 5 d in 3D Matrigel culture in the presence or absence of NS-398 as shown in Figure 2. Cells were fixed and then exposed to TUNEL stain. Representative fields are shown with TUNEL-positive cells stained in green. The majority of fields of K-Ras cells showed no TUNEL-positive cells. (B) Extracts were prepared from each of the cell populations and immunoblotted for cleaved caspase-3. Results are representative of three independent experiments.

MATERIALS AND METHODS

Reagents

The following antibodies were used in this study: monoclonal antibody against E-cadherin, C36, was from BD Biosciences (Franklin Lakes, NJ); 4A2C7 was from Invitrogen (Carlsbad, CA); H108 anti-human E-cadherin antibody was from Santa Cruz Biotechnology (Santa Cruz, CA). Antibodies against ERKs, phospho (p)-ERKs, AKT, p-AKT, β-catenin, p-β-catenin, and cleaved caspase-3, all were from Cell Signaling Technology (Beverly, MA); COX-2 antibody was from Cayman Chemical (Ann Arbor, MI); and β-actin antibody was from Sigma-Aldrich (St. Louis, MO). All signaling inhibitors were from Calbiochem (San Diego, CA). TOPFLASH, FOPFLASH, and dominant-negative T cell factor (TCF) plasmids were provided by Dr. Robert Winn (Department of Medicine, University of Colorado, Denver, CO). All other reagents were from Sigma-Aldrich.

Cell Two-dimensional (2D) and Three-dimensional (3D) Culture

RL-65 cells were cultured in RL-65 growth medium with 7% bovine pituitary extract (BPE) at 37°C, 5% CO_2. K-Ras–transfected cells were prepared using retroviral-mediated gene transfer as described previously (Blaine *et al.*, 2001). For 2D cultures, cells were plated at 5000 cells/ml into eight-well chamber slides and grew 3 d for colony formation. For 3D culture, cells were imbedded in RL-65 cell growth medium with 4% Matrigel and evaluated at day 5 and day 8 as described previously (Bren-Mattison *et al.*, 2005). Protein extracts from 3D cultures were prepared by treating cultures with Dispase to digest the Matrigel. Cell suspensions were then washed with phosphate-buffered saline (PBS), and lysates were prepared as described below.

PGE$_2$ Enzyme-linked Immunosorbent Assay (ELISA)

Cells were treated in the presence or absence of NS-398 (10 μM) in growth medium for 48 h. Then, cells were switched to BPE-free medium to release PGE$_2$ from the cells for 2 h. Cell medium was collected and normalized for total cell protein, and the level of PGE$_2$ was measured by a PGE$_2$ enzyme immunoassay kit from Cayman Chemical (Ann Arbor, MI), following the instructions from the manufacturer.

Gelatin Zymography Assay

Cells were lysed in MAPK lysis buffer containing 1% Triton X-100 and normalized with protein concentration. Samples were added to sample buffer without reducing reagents. Proteins were separated by 10% zymogram gel. The gel was incubated with renaturing buffer at room temperature for 30 min, followed by incubation with developing buffer at 37°C overnight. The gel was stained with Simply blue, and the gelatinolytic activities were detected as clear bands against a blue background.

Cell Proliferation Assay

Cells were seeded at density of 500 cell/well into 96-well cell culture plates in BPE-free medium. Cells were grown for 72 h. Live cells were quantified by CellTiter 96 Aqueous One Solution Cell Proliferation Assay (Promega, Madison, WI) by following the manufacturer's protocol. The OD values were converted into cell numbers by a cells/OD standard curve.

Preparation of Cytoplasmic and Nuclear Protein

Soluble cytoplasmic and nuclear protein were prepared by using Nuclear Extract kit from Active Motif (Carlsbad, CA). Briefly, cells were washed with cold PBS and removed from dishes with cell lifter. Cell pellets were resuspended into 500 μl of hypotonic buffer and incubated on ice for 15 min. Then, 25 μl of detergent was added to each tube and vortexed for 10 s. After centrifugation, the supernatants were collected as cytoplasmic protein. Nuclear pellets were resuspended in 50 μl of Complete lysis buffer and incubated on ice for 30 min. The supernatants were collected as nuclear protein after centrifuging at $14,000 \times g$ for 10 min at 4°C. The protein concentration was measured in cytoplasmic portion and was used to normalize the nuclear proteins. Equal amounts of protein were loaded on SDS-polyacrylamide gel electrophoresis (PAGE) followed by immunoblotting.

Immunoprecipitation and Immunoblotting

Cells were lysed in MAPK lysis buffer at 4°C for 1 h. Supernatants of cell lysates were normalized with protein concentration and immunoprecipitated with primary antibody at 1–1.25 μg/tube at 4°C for 2 h. Then, 50 μl of protein G was added and incubated for another hour. SDS-PAGE was carried out as described previously, and proteins were separated on the gel were transferred to a polyvinylidene difluoride membrane. After blocking with 3%

fat-free dry milk in Tris-buffered saline, the membrane was probed with primary antibody. The membranes were further probed with horseradish peroxidase-conjugated goat anti-rabbit or rabbit anti-mouse immunoglobulin for 1 h at room temperature. Antibody binding was visualized by enhanced chemiluminescence.

Transepithelial Resistance (TER) Measurements

TER was measured as described previously (Lanaspa *et al.*, 2007), using an EVOM apparatus (WPI, Sarasota, FL). Cells were plated at 2×10^5 into 24-well transwell filters (1-μm pore size; Millipore, Billerica, MA) in growth medium. After overnight incubation, cells were switched to fresh medium and followed by TER measurement immediately. TER was calculated by subtracting the resistance of a blank filter multiplied by the area of the monolayer. Results are shown as the mean of three independent measurements for each cell line.

RNA Isolation and Real-Time Reverse Transcription-Polymerase Chain Reaction (RT-PCR)

Total RNA was isolated using the RNeasy kit (QIAGEN, Valencia, CA), and its concentration was determined by OD 260/280. First-strand cDNA was synthesized with 2 μg of total RNA (DNase-treated) in a 20-μl reverse transcriptase reaction mixture using iSCRIPT cDNA synthesis kit from Bio-Rad (Hercules, CA). All real-time PCR reactions were performed in a 25-μl mixture containing 1/10 volume of cDNA preparation (2.5 μl), 1× SYBR Green buffer (Sigma-Aldrich), and 0.2 μM each primer. The sequences of MMP-9 (rat) primers are as follows: forward, ttc gac gct gac aag aag tg and reverse, agg gga gtc ctc gtg gta gt. The internal control of 18S primers were from Applied Biosystem (Foster city, CA). Real-time quantitations were performed using the iCycler iQ system (Bio-Rad). The fluorescence threshold value was calculated using the iCycle iQ system software.

Immunostaining and Image Analysis

Cells were set up in chamber slides as described in *Results*. Cells were fixed in 2% paraformaldehyde-PBS for 15 min at room temperature. Cells were permeabilized with 0.5% Triton X-100 for 15 min if needed. All samples were blocked with 1% bovine serum albumin (BSA) in PBS for 1 h at room temperature. Cells were incubated with primary antibody for 2 h at room temperature, or overnight at 4°C for 3D culture, followed by 1-h incubation with appropriate secondary antibodies. Slides were mounted and viewed with a TE2000-S IF microscope (Nikon, Tokyo, Japan) or a 510 Meta/FCS laser-scanning confocal microscope (Carl Zeiss, Thronwood, NY). Confocal image stacks were processed using LSM Image Examiner (Carl Zeiss).

Terminal Deoxynucleotidyl Transferase dUTP Nick-End Labeling (TUNEL) Assay

The TUNEL assay was performed with the TUNEL apoptosis detection kit from Upstate Cell Signaling Solutions (Temecula, CA), by following the manufacturer's protocol. RL-65 cells were cultured for 3 d in eight-well chamber slides at a density of 2000 cells/well, with or without 20 μM NS-398 in growth medium. Cells were fixed in 4% paraformaldehyde in PBS for 15 min at room temperature and then permeabilized with 0.5% Tween 20, 0.2% BSA in PBS for 15 min. Cells were incubated with terminal deoxynucleotidyl transferase end-labeling cocktail for at least 60 min at room temperature. After blocking with block buffer for 15 min, fluorescence was developed by incubating with Avidin-fluorescein isothiocyanate solution for 30 min. Nuclei were counterstained with 4,6-diamidino-2-phenylindole. The TUNEL-positive cells were checked with a TE2000-S IF microscope.

Luciferase Reporter Gene Assay

RL-56 cells were seeded in 60-mm dishes at 1×10^6 cells/dish overnight. Plasmids linked to a luciferase reporter (TOPFLASH, COX-2 promoter) were transiently transfected with 0.5 μg of β-galactosidase (β-Gal) by lipofectin. After 4-h incubation, cells were switched back to growth medium. For studies of pharmacological inhibitors, agents were added 24 h after transfection, and cells were harvested 48 h later. Cells were lysed in luciferase Reporter Lysis buffer, and supernatants of cell lysates were subjected to luciferase and β-Gal activity as described previously (Van Putten *et al.*, 2001).

RESULTS

K-Ras Expression Effects on Increased Proliferation and Delayed Formation of Acinar Structures in Three-dimensional Culture Are Mediated by COX-2

To evaluate the impact of oncogenic K-Ras on nontransformed lung epithelial cells, we stably transfected RL-65 cells, a nontransformed lung epithelial cell line (Roberts *et al.*, 1990), with oncogenic K-Ras (K-Ras^{G12V}). RL-65 cells

were chosen because they represent a spontaneously immortalized cell line, have high levels of E-cadherin expression, form a high-resistance epithelium in two-dimensional tissue culture, and form hollowed-out acinar structures in three-dimensional Matrigel cultures (Bren-Mattison *et al.*, 2005). To validate functional expression of K-Ras, cells were evaluated for activation of downstream signaling pathways. Expression of oncogenic K-Ras resulted in increased activation of ERK as assessed by immunoblotting for phospho-ERK, and activation of PI3-kinase/Akt pathway, as determined by increased levels of phospho-Akt (Figure 1A). We and others have reported previously that activation of H-Ras induces expression of COX-2 and increases PGE$_2$ production (Van Putten *et al.*, 2001). Expression of oncogenic K-Ras also resulted in a marked increase in COX-2 expression (Figure 1A) and elevated levels of PGE$_2$ (Figure 1B); the increased PGE$_2$ production was blocked by treatment of cells with NS-398, a COX-2–specific inhibitor. Although all inhibitors may have "off-target" effects, this agent seems to be highly selective for COX-2, and it failed to activate peroxisome proliferator-activated receptor γ in these cells (data not shown).

We examined effects of K-Ras on cell proliferation. In the absence of growth factors (−BPE), K-Ras cells showed almost a twofold increase in cell proliferation compared with empty vector controls (Figure 2A). This increase was com-
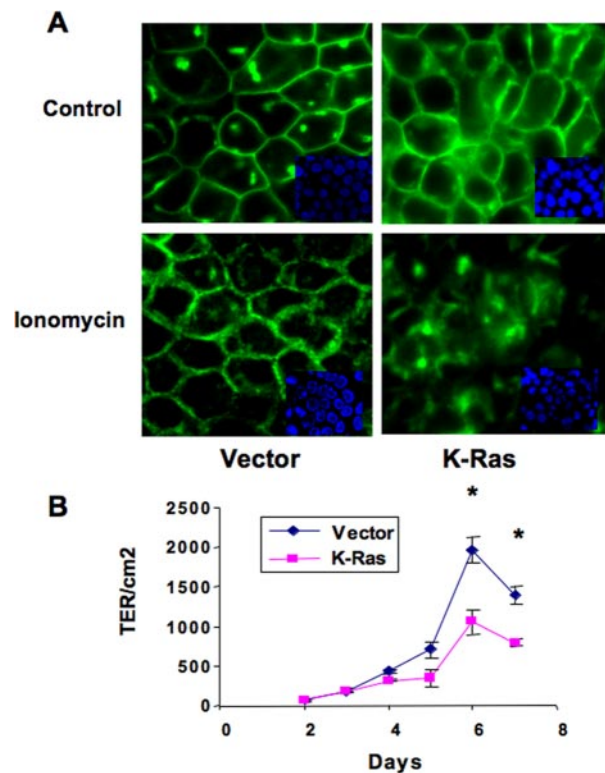

Figure 4. K-Ras lowers adherens junctions and transepithelial resistance. (A) Cells were plated on eight-well chamber slides and grown for 48 h to achieve a confluent monolayer, and then they were treated with 5 μM ionomycin or vehicle (control) for 30 min at 37°C. Cells were then fixed and stained with anti-E-cadherin antibody to view cell adherens junctions. Representative pictures shown are from three independent experiments. (B) Cells were plated at a density of 50,000 cells/transwell in growth medium overnight. Then cells were switched to BPE-free medium and TER was measured daily, as described in *Materials and Methods*. Data represent the mean from four independent experiments. *p < 0.05 versus K-Ras.
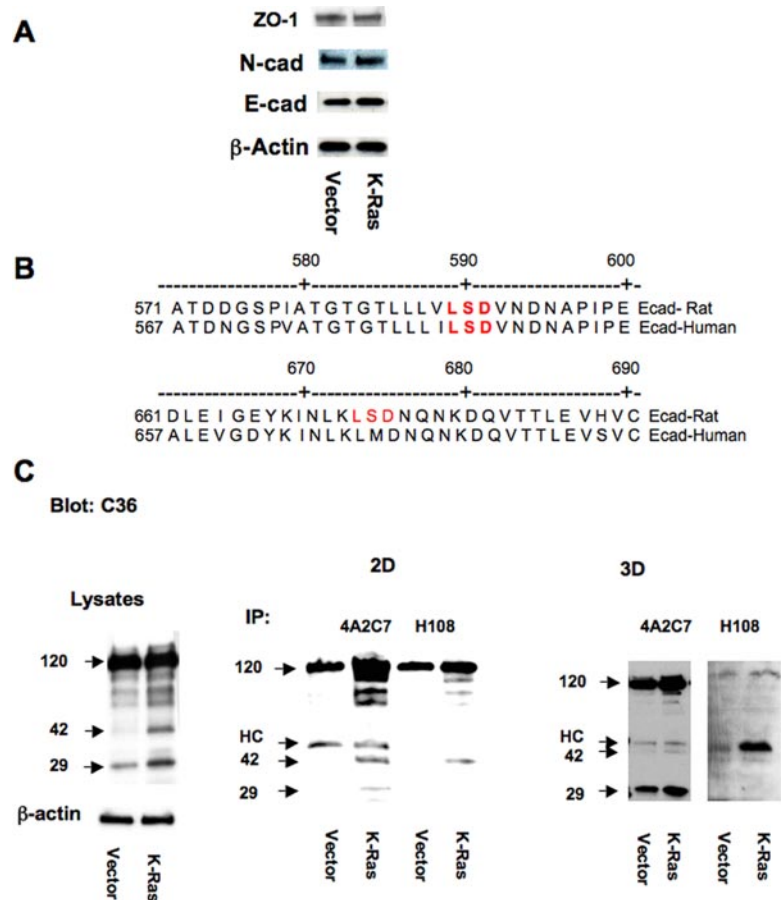
Figure 5. K-Ras promotes E-cadherin shedding. (A) Cell lysates from vector control and K-Ras cells were immunoblotted with the indicated antibodies. (B) Sequence analysis of MMP-9 LSD cutting sites in both human and rat E-cadherin. (C) Cell lysates prepared from vector control (V) or K-Ras–transfected (K) cells were immunoprecipitated with two anti-E-cadherin antibodies, 4A2C7 and H108, and the immunoprecipitates were immunoblotted with another specific antibody that recognizes the carboxy terminal of the molecule (C36). Arrows indicate predicted specific cleavage products at 42 and 29 kDa. The 120-kDa band represents full-length E-cadherin. HC, immunoglobulin G heavy chain.

pletely blocked by treating cells with the COX-2 inhibitor NS-398. We also determined whether expression of K-Ras was sufficient to cause transformed growth as assessed by colony formation in soft agar. Consistent with findings of other investigators (Sato *et al.*, 2006), K-Ras cells failed to form any colonies in soft agar (data not shown). Growth was also examined in three-dimensional Matrigel cultures. To assess acinar formation, equal numbers of K-Ras and vector control cells were plated in Matrigel and followed as a function of time. Confocal analysis of acini stained with anti-E-cadherin antibodies revealed that vector control cells formed acinar structures containing a hollow lumen formed by day 5 (Figure 2B, top left), and the hollow rate increased over time (Supplemental Figure 1). K-Ras–expressing cells consistently formed larger structures, but the rate of lumen formation, defined by hollowing out of the structures was markedly delayed (Figure 2B, bottom left). We quantified both acinar size and percentage of hollowing out at both 5 and 8 d after plating. At 5 d, acini from K-Ras cells were approximately twice as large (Figure 2C) compared with vector control cells. Acini from vector cells started to hollow out at day 3; ~60% of acini were hollowed by day 5 (Figure 2D) and 100% by day 8 (Supplemental Figure 1). In K-Ras cells, only 16% of acini were hollow at day 5 (Figure 2D), and 40% at day 8 (data not shown). Exposure of cells to NS-398 had no significant effect on either acinar size or the extent of hollowing out in vector control cells but significantly decreased acinar size and increased the rate of hollowing out in K-Ras–transfected cells (Figure 2, B–D).

The formation of hollow structures in 3D culture has been attributed to apoptosis of cells that are not in contact with the extracellular matrix. We therefore examined the effects of K-Ras on apoptosis. Apoptosis was assessed in both 2D and 3D cultures by TUNEL staining. The appearance of TUNEL-positive cells was decreased in K-Ras–transfected cells compared with vector controls in both 2D and 3D cultures (Figure 3A). Exposure of K-Ras cells to NS-398 increased the number of TUNEL-positive cells under both culture conditions. Exposure of vector control cells to NS-398 had no significant effect on apoptotic nuclei. To confirm changes in apoptosis, expression of active caspase-3 was examined by immunoblotting. Levels of cleaved caspase-3 were lower in K-Ras–transfected cells compared with vector controls, both in 2D and 3D culture (Figure 3B). NS-398 exposure had no significant effect on cleaved caspase-3 levels in vector control cells, but increased activated caspase-3 levels in K-Ras cells to levels comparable with those seen in vector controls. From these data, we conclude that K-Ras expression reduces apoptosis in RL-65 cells and that this is mediated through a COX-2–dependent pathway.

K-Ras Leads to Altered Epithelial Morphology

Because K-Ras has been implicated in modulating epithelial–mesenchymal transitions, we studied the epithelial nature of K-Ras cells in more detail. Cell morphology was examined by immunofluorescent staining with anti E-cadherin antibody. As seen in Figure 4A, vector control cells showed a cobblestone-like morphology, with positive staining of E-cadherin localized to cell junctions. K-Ras–transfected RL-65 cells looked smaller as determined by flow cytometry (data not shown), and they formed tightly packed colonies with increased nuclear/cytoplasmic ratio. E-cad-

herin staining in K-Ras cells was still localized to areas of cell–cell contact, but it was more diffuse, suggesting a partial breakdown of adherens junctions (Figure 4A, top). To further assess the stability of these junctions, cells were treated with 5 μM ionomycin for 30 min. Although ionomycin through increases in intracellular Ca^{2+} will have multiple effects on cells, studies have demonstrated specific effects on disruption of adherens junctions (Ito *et al.*, 1999). In vector control cells, ionomycin treatment resulted in more diffuse E-cadherin staining, indicating that E-cadherin contacts were altered, but the adherens junction structure remained intact. However, in K-Ras–transfected cells, ionomycin resulted in complete disruption of cell–cell contacts (Figure 4A, bottom).

Changes in the integrity of tight junctions were confirmed by measuring TER. Cultures were grown on transwell filters, and resistance was measured as a function of time. TER reached maximal values at day 6 and started to decline by day 7. K-Ras cells had consistently lower values of TER throughout the course of the experiment (Figure 4B). At the time of maximal TER, K-Ras cells had 42% of the value seen in vector control cells. It should be noted that the TER values in K-Ras cells were still significant compared with nonepithelial cells, consistent with a partial loss of adherens junctions.

K-Ras Increases E-cadherin Shedding from Cell Surface, Which Is Mediated by MMP-9

To determine whether these changes in cell adhesions were mediated by altered expression of adhesion proteins, extracts from vector control and K-Ras cells were immunoblotted for E-cadherin, N-cadherin, and zona occludens (ZO)-1. As shown in Figure 5A, no differences were observed in protein expression for any of these proteins. Changes in E-cadherin transcription were assessed by transiently transfecting cells with a construct encoding the E-cadherin promoter driving a luciferase reporter. Expression of K-Ras had no effect on E-cadherin promoter activity (data not shown), consistent with the lack of change in protein expression.

Several studies have demonstrated that shedding of E-cadherin's ectodomain by proteolytic cleavage occurs in other cell types, which results in disrupting of cell–cell contacts and β-catenin redistribution (Ito *et al.*, 1999; Maretzky *et al.*, 2005; Symowicz *et al.*, 2007). Human E-cadherin is cleaved at a specific lysine-serine-aspartic acid (LSD) sequence in the extracellular domain, resulting in a shed 80-kDa ectodomain and a membrane-associated 38-kDa fragment (Ito *et al.*, 1999). Examination of the rat E-cadherin sequence indicates that there are two LSD sequences in the extracellular portion of the molecule. One of these is conserved in human cells, but the other is not. Based on this, we would predict that cleavage at LSD sites would result in two fragments, of 42 and 29 kDa (Figure 5B). To evaluate E-cadherin shedding in RL-65 cells, lysates were immunoprecipitated with two E-cadherin antibodies, 4A2C7 and H108, and the immunoprecipitates immunoblotted with a specific antibody that recognizes the carboxy terminus of the molecule (C36). We consistently observed two bands at the predicted sizes of 42 and 29 kDa (Figure 5C). The intensity of both of these bands was increased as a function of time after plating (data not shown); and importantly, extracts from K-Ras cells had increased levels of both of these bands at all times examined. Similar increases in cleavage products were also observed in extracts derived from cells grown in 3D culture (Figure 5C, right). We attempted to use antibodies against the amino terminal of the E-cadherin to determine whether the 80-kDa ectodomain could be identified in media from RL-65 cells. However, the HECD antibody used by
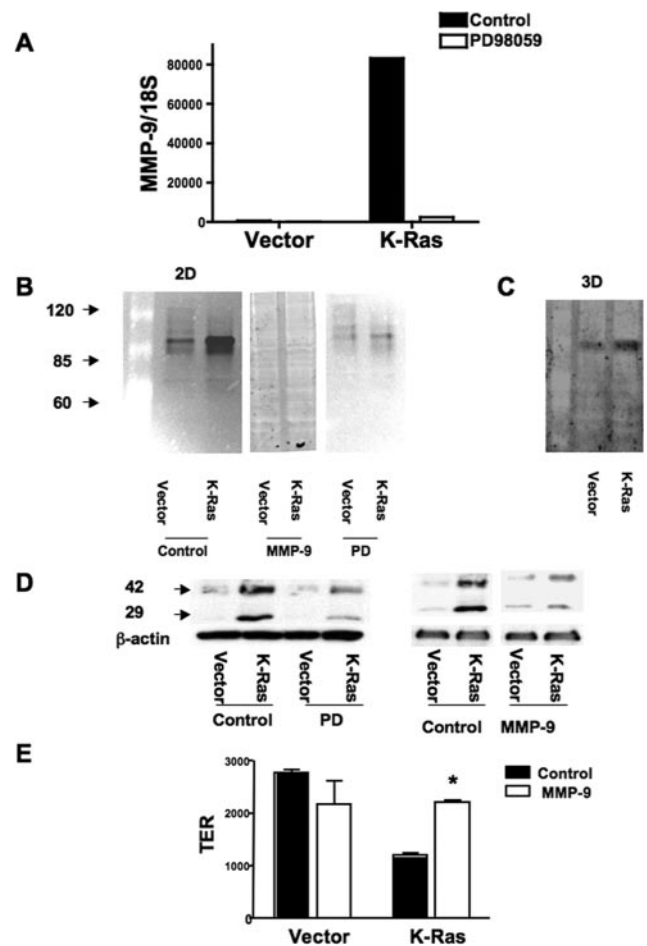

Figure 6. E-cadherin shedding is mediated by increased MMP-9 activity. (A) The indicated cells were treated overnight with PD 98059 (50 μM) or vehicle (control). Total RNA was isolated and expression of MMP-9 mRNA normalized to 18S determined by quantitative RT-PCR. Data are representative of three independent experiments. (B) Cell were treated with PD 98059 or vehicle, and cell lysates were prepared in MAPK lysis buffer. MMP-9 activity was detected by zymography as described in *Materials and Methods*. Separate lysates were harvested and pretreated with MMP-9 inhibitor before being run on zymography gels. (C) Lysates were isolated from 3D cultures of vector control and K-Ras cells. Extracts were analyzed for MMP-9 activity as in A. (D) The indicated cells were treated with either 50 μM PD98059 or 20 μM MMP-9 inhibitor overnight. Lysates were immunoblotted with the C36 anti-E-cadherin antibody. Both inhibitors significantly reduced E-cadherin cleavage. (E) Confluent dishes of vector or K-Ras cells were treated overnight with the MMP-9 inhibitor or vehicle and TER measured as in Figure 5. MMP-9 Inhibitor increased TER only in K-Ras cells.

other investigators in human cells (Symowicz *et al.*, 2007), failed to detect the rat E-cadherin in immunoblotting of cell lysates (data not shown) and does not seem to recognize the rat form of the molecule.

Cleavage of E-cadherin has been reported to be mediated by metalloproteinases such as MMP-9 (Ito *et al.*, 1999) as well as a disintegrin and metalloproteases (Maretzky *et al.*, 2005; Symowicz *et al.*, 2007). Levels of candidate MMPs were examined in RL-65 cells. Expression of MMP-9 mRNA was markedly increased in RL-65 expressing K-Ras compared with LNCX vector controls (Figure 6A). This increase was completely blocked by treatment of cells with the MEK inhibitor PD 98059. MMP-9 activity was measured in cell

Figure 7. Effects of COX-2 and MMP-9 on β-catenin signaling. (A) Vector control or K-Ras cells were transfected with TOPFLASH promoter construct along with a plasmid encoding β-Gal under the control of the cytomegalovirus promoter to normalize for transfection efficiency. After recovering overnight, cells were treated for 24 h with vehicle (control), 10 μM NS-398, 10 μM PGE$_2$, or both NS-398 and PGE$_2$ (NS+PGE$_2$) for 24 h. Normalized TOPFLASH activity was determined. Results represent the means of three independent experiments performed in triplicate. *p < 0.05 versus vector; **p < 0.05 versus K-Ras. (B) Cells were transfected as described in A and then treated with either vehicle (control), 50 μM PD 98059, or 20 μM MMP-9 Inhibitor, or cotransfected with an expression plasmid for DN-TCF. *p < 0.05 versus vector; **p < 0.05 versus K-Ras. (C) Cell lysates were harvested from vector control or K-Ras cells and immunoblotted for either phosphorylated GSK-3β or total GSK-3β. K-Ras cells had elevated levels of phosphorylated GSK-3β. Results are representative of three independent experiments. (D) Vector control and K-Ras cells were exposed for 24 h to the indicated agents. Cells were harvested and cytoplasmic and nuclear fractions isolated as described in *Materials and Methods*. Lysates were normalized with protein and immunoblotted for total β-catenin (β-Cat). Levels of β-actin were used as a loading control. Results are representative of three independent experiments. (E) Vector control or K-Ras cells were transfected with a plasmid encoding a dominant-negative TCF (DN-TCF). Cells were incubated for 72 h after transfection, and cell numbers were determined. Expression of DN-TCF inhibited cell growth only in K-Ras–expressing cells. Results are the mean of three independent experiments. *p < 0.05 versus vector control; **p < 0.05 versus K-Ras control.
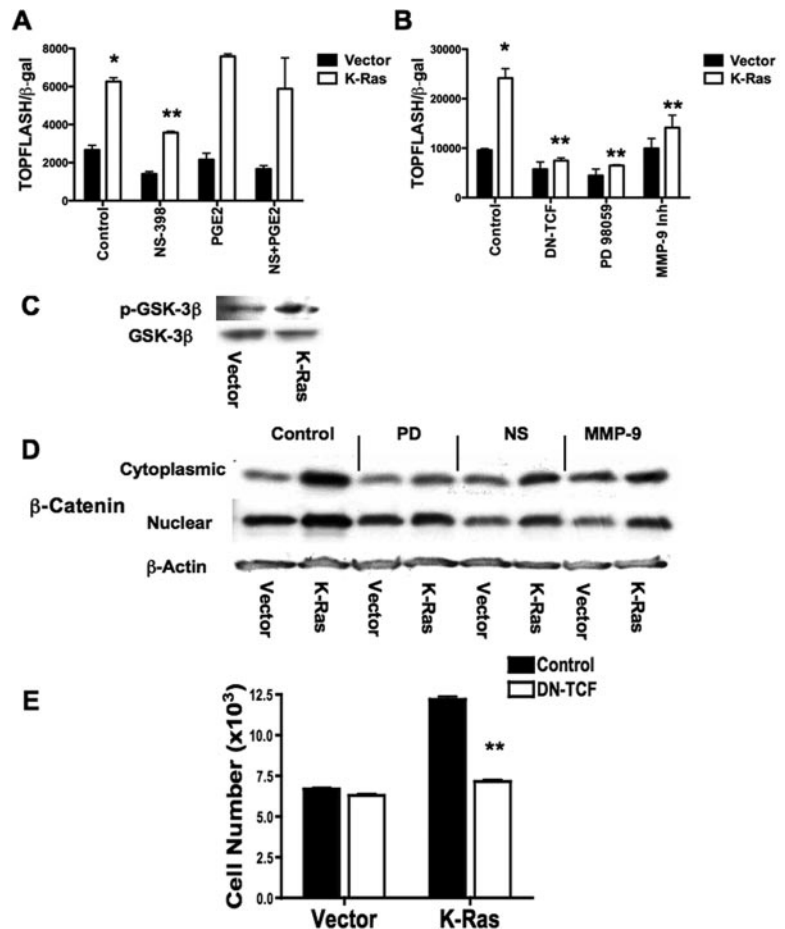
lysates by gelatin zymography (Jorda *et al.*, 2005). A single band at ~90 kDa was detected, corresponding to the molecular weight of MMP-9. Gelatinase activity was markedly increased in extracts from K-Ras cells, and this activity was abolished by treatment of cells with PD 98059 (Figure 6B). Activity was also increased in extracts prepared from cells grown in 3D culture (Figure 6C). To test the role of MMP-9 in E-cadherin processing, cells were treated with a MMP-2/MMP-9 inhibitor (MMP-2/MMP-9 inhibitor III). Treatment of K-Ras cells with either PD 98059 or the MMP inhibitor blocked E-cadherin cleavage (Figure 6D) and completely inhibited MMP-9 activity as assessed by zymography (Figure 6B). The MMP-9 inhibitor also largely restored the TER seen in K-Ras cells to levels seen in empty vector controls (Figure 6E). We attempted to assess the effects of PD 98059 on TER, but incubation of confluent monolayers with this agent resulted in detachment of some cells, which drastically lowered the TER measurements. This is consistent with growth inhibitory effects of PD 98059 observed in these cells (data not shown). We also tested the role of COX-2 on MMP-9 activation and E-cadherin shedding. Treatment of cells with NS-398 for up to 3 d had no effect the ability of K-Ras to increase MMP-9 activity or promote E-cadherin shedding (data not shown).

K-Ras Signals through Stabilization of β-Catenin
Signaling through the canonical Wnt pathway inhibits β-catenin phosphorylation, resulting in increased levels of β-catenin, which then can translocate to the nucleus and

increase TCF-dependent gene expression (Gordon and Nusse, 2006). Recent studies have demonstrated that PGE$_2$ signaling through the EP2 receptor can inhibit glycogen synthase kinase (GSK)-3–mediated phosphorylation of β-catenin (Castellone *et al.*, 2005), resulting in activation of β-catenin–dependent gene expression. Because K-Ras induces expression of COX-2, we examined the role of COX-2 on β-catenin–mediated signaling, by measuring TCF-dependent gene expression with the TCF-dependent TOPFLASH promoter construct. K-Ras cells had increased TOPFLASH activity, and this increase was inhibited by NS-398 (Figure 7A). Addition of exogenous PGE$_2$ reversed the effects of NS-398 on TOPFLASH activity (Figure 7A). TOPFLASH activity was also inhibited by the MEK inhibitor PD 98059 as well as the MMP-9 inhibitor (Figure 7B). Consistent with a previous study (Castellone *et al.*, 2005), K-Ras cells demonstrated higher levels of phosphorylated (inactivated) GSK-3β (Figure 7C). To confirm that these effects are mediated by changes in β-catenin levels, we determined levels of cytoplasmic and nuclear β-catenin in vector control and K-Ras cells. Consistent with measurements of TOPFLASH activity, K-Ras cells had increased levels of β-catenin (Figure 7D). Treatment with either PD 98069, NS-398, or the MMP-9 inhibitor inhibited the increased expression of β-catenin both in the cytoplasm and in the nuclear fraction of K-Ras cells but had little effect on β-catenin levels in vector control cells (Figure 7D). Finally, expression of a dominant-negative TCF construct, which inhibited TOPFLASH activity (Figure
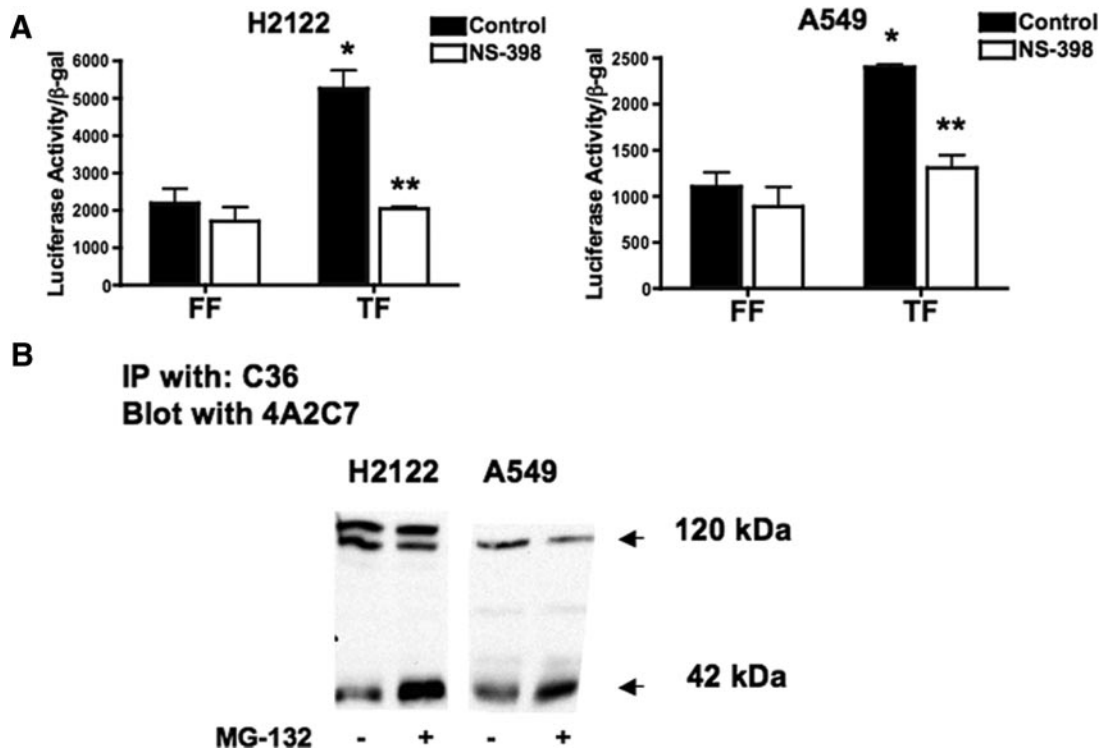
Figure 8. TOPFLASH and E-cadherin cleavage in human NSCLC expressing oncogenic K-Ras. (A) H2122 (left) and A549 cells (right) were transiently transfected with TOPFLASH (TF) or FOPFLASH (FF) promoter as a negative control. After transfection, cells were with NS-398 or vehicle (control) for 24 h, and promoter activity was normalized to β-gal determined. NS-398 decreased TOPFLASH in both cell lines. (B) E-cadherin shedding occurs in both cell lines. The 42-kDa E-cadherin fragment was detected in anti-E-cadherin immunoprecipitations followed by immunoblotting with a different E-cadherin antibody.

7B), blocked the increased proliferation seen in K-Ras cells (Figure 7E).

Activation of β-Catenin Pathway and E-cadherin Shedding Occurs in NSCLC Expressing Oncogenic K-Ras

Most NSCLC cell lines are characterized by a loss of epithelial features. This is mediated by oncogenic signaling pathways that regulate expression of epithelial markers such as E-cadherin. To determine whether the effects seen with K-Ras in nontransformed RL-65 cells are also observed in NSCLC expressing K-Ras, we examined two adenocarcinoma cell lines, H2122 and A549. Both of these cells lines express high levels of COX-2 and produce PGE$_2$ (Heasley *et al.*, 1997). TOPFLASH activity was expressed in both cell lines (Figure 8A). In both cell lines, treatment with NS-398 inhibited TOPFLASH activity. E-cadherin cleavage was examined by immunoblotting. In both cell lines, we detected a specific E-cadherin cleavage product of the predicted size of 42 kDa, using immunoprecipitation, followed by immunoblotting with a different antibody (Figure 8B). In some cell types, initial cleavage products of E-cadherin generated by MMPs are rapidly degraded by intracellular proteases; therefore, several studies have treated cells with MG132, a general inhibitor of intracellular proteases to allow easier detection of specific MMP cleavage products (Ito *et al.*, 1999). Treating NSCLC with this agent increased the intensity of the 42-kDa cleavage product.

DISCUSSION

The prevalence of K-Ras mutations in NSCLC suggests that it is a dominant signaling pathway critical for transforma-

tion of lung epithelial cells. However, transformation of epithelial cells requires multiple events, including activation of oncogenic pathways, and inhibition of tumor suppressor activity (Hamad *et al.*, 2002). Although the signaling pathways engaged by Ras have been extensively studied, less is known regarding effects of Ras signaling on the properties of nontransformed epithelial cells. In this study, we have examined the effects of K-Ras on the properties of a spontaneously immortalized lung epithelial cell line, RL-65. We chose these cells because they possess the properties of highly differentiated epithelial cells. These include cobblestone morphology, a high transepithelial resistance indicative of tight and adherens junctions, and the ability to form hollowed out acinar structures in 3-D Matrigel culture. Our data indicate that activation of the ERK pathway, which is constitutively elevated in the setting of K-Ras expression is a critical mediator of the observed biological responses. Previously, we have shown that ERK activation is critical for transcriptional induction of COX-2 and elevated production of PGE$_2$ in these cells (Van Putten *et al.*, 2001). In the current study, we have demonstrated that PGE$_2$, through its receptor(s) leads to enhanced proliferation through activation of the β-catenin pathway, and an impairment in formation of hollow acinar structures by inhibiting apoptosis. These findings are recapitulated in NSCLC expressing K-Ras, where cells form organized acinar structures, but fail to hollow out (Bren-Mattison *et al.*, 2005). Simultaneously, ERK activation is critical for the induction of MMP-9 through a COX-2-independent pathway. Increased expression and consequently enzymatic activity of MMP-9 contributes to the cleavage of E-cadherin to release an ectodomain, and disruption of adherens junctions, with a concomitant decrease

in epithelial resistance. Although inhibition of MMP-9 reverses the decrease in epithelial resistance seen with K-Ras, it is likely that alterations of tight junctions are not mediated exclusively through MMP-9 but are likely to involve other proteinases. Inhibiting MMP-9 activity does reverse the increased soluble and nuclear β-catenin seen with K-Ras expression and inhibits TOPFLASH, suggesting that E-cadherin cleavage disrupts E-cadherin/β-catenin interactions at the plasma membrane. We therefore propose a model in which ERK-mediated COX-2 and MMP-9 induction cooperate to increase β-catenin signaling. COX-2 results in inhibition of β-catenin phosphorylation and stabilization of the protein, whereas MMP-9 releases β-catenin from membrane complexes.

Expression of oncogenic K-Ras is not sufficient to transform RL-65, because these cells do not form colonies in soft agar. Studies by Dr. Minna and coworkers have demonstrated that multiple events are required for transformation of human bronchial epithelial cells (Sato *et al.*, 2006). In breast epithelial cells, studies have shown that H-Ras and transforming growth factor (TGF)-β signaling can cooperate and lead to transformation of cells that form tumors in nude mice (Oft *et al.*, 1996). Furthermore, these workers have demonstrated that these two pathways impinge on degradation of E-cadherin to promote EMT (Janda *et al.*, 2006). We have examined the effects of TGF-β in K-Ras-expressing RL-65 cells, but we have not observed either the morphological changes observed in breast epithelial cells, nor the formation of colonies in soft agar. Thus, the pathways that collaborate with Ras remain to be identified. From the present study, we conclude that activated Ras increases cell proliferation and causes quantitative changes in epithelial contacts. However, cell junctions, although partially disrupted are still functional, and the cells do not undergo EMT. To achieve the properties of a cancer cell it is likely that a more complete disruption of cell junctions is required, to allow cells to proliferate in an anchorage-independent manner. This may require altered protein expression of E-cadherin, and other cell junction proteins, which is not observed in the setting of K-Ras. The Snail family of transcription factors have been implicated in mediating EMT and transformation, at least in part through suppression of E-cadherin expression (Peinado *et al.*, 2007). Pathways that target these transcription factors represent potential signals that will collaborate with Ras to lead to transformation of lung epithelial cells.

In summary, our study demonstrates that oncogenic Ras signaling initiates many of the properties seen in full-fledged cancer cells, including increased proliferation, decreased apoptosis, impaired cell–cell contacts, and up-regulation of MMPs. These effects are mediated in large part through increased ERK activity and increased production of prostaglandins as a consequence of COX-2 induction. Finally, our studies indicate that lung epithelial cells seem to be more resistant to undergoing transformation compared with breast epithelial cells. Recent studies have suggested that nontransformed breast epithelial cells lines contain a subpopulation of "stem cell line" mesenchymal cells (Mani *et al.*, 2008). It will be of interest to determine whether the relative resistance of lung epithelial cells to transformation is related to the absence of such a population of stem-like cells.

ACKNOWLEDGMENTS

REFERENCES

Blaine, S. A., Wick, M., Dessev, C., and Nemenoff, R. A. (2001). Induction of cPLA2 in lung epithelial cells and non-small cell lung cancer is mediated by Sp1 and c-Jun. J. Biol. Chem. *276*, 42737–42743.

Bollag, G., Adler, F., elMasry, N., McCabe, P. C., Conner, E. Jr., Thompson, P., McCormick, F., and Shannon, K. (1996). Biochemical characterization of a novel KRAS insertion mutation from a human leukemia. J. Biol. Chem. *271*, 32491–32494.

Bren-Mattison, Y., Van Putten, V., Chan, D., Winn, R., Geraci, M. W., and Nemenoff, R. A. (2005). Peroxisome proliferator-activated receptor-gamma (PPAR(gamma)) inhibits tumorigenesis by reversing the undifferentiated phenotype of metastatic non-small-cell lung cancer cells (NSCLC). Oncogene *24*, 1412–1422.

Campbell, S. L., Khosravi-Far, R., Rossman, K. L., Clark, G. J., and Der, C. J. (1998). Increasing complexity of Ras signaling. Oncogene *17*, 1395–1413.

Castellone, M. D., Teramoto, H., Williams, B. O., Druey, K. M., and Gutkind, J. S. (2005). Prostaglandin E2 promotes colon cancer cell growth through a Gs-axin-beta-catenin signaling axis. Science *310*, 1504–1510.

Dannenberg, A. J., Altorki, N. K., Boyle, J. O., Dang, C., Howe, L. R., Weksler, B. B., and Subbaramaiah, K. (2001). Cyclo-oxygenase 2, a pharmacological target for the prevention of cancer. Lancet Oncol. *2*, 544–551.

Gordon, M. D., and Nusse, R. (2006). Wnt signaling: multiple pathways, multiple receptors, and multiple transcription factors. J. Biol. Chem. *281*, 22429–22433.

Halbleib, J. M., and Nelson, W. J. (2006). Cadherins in development: cell adhesion, sorting, and tissue morphogenesis. Genes Dev. *20*, 3199–3214.

Hamad, N. M., Elconin, J. H., Karnoub, A. E., Bai, W., Rich, J. N., Abraham, R. T., Der, C. J., and Counter, C. M. (2002). Distinct requirements for Ras oncogenesis in human versus mouse cells. Genes Dev. *16*, 2045–2057.

Heasley, L. E., Thaler, S., Nicks, M., Price, B., Skorecki, K., and Nemenoff, R. A. (1997). Induction of cytosolic phospholipase A_2 by oncogenic Ras in human non-small cell lung cancer. J. Biol. Chem. *272*, 14501–14504.

Horio, Y., Chen, A., Rice, P., Roth, J. A., Malkinson, A. M., and Schrump, D. S. (1996). Ki-*ras* and *p53* mutations are early and late events, respectively, in urethane-induced pulmonary carcinogenesis. Mol. Carcinog. *17*, 217–223.

Huber, M. A., Kraut, N., and Beug, H. (2005). Molecular requirements for epithelial-mesenchymal transition during tumor progression. Curr. Opin. Cell Biol. *17*, 548–558.

Ito, K., Okamoto, I., Araki, N., Kawano, Y., Nakao, M., Fujiyama, S., Tomita, K., Mimori, T., and Saya, H. (1999). Calcium influx triggers the sequential proteolysis of extracellular and cytoplasmic domains of E-cadherin, leading to loss of beta-catenin from cell-cell contacts. Oncogene *18*, 7080–7090.

Janda, E., Nevolo, M., Lehmann, K., Downward, J., Beug, H., and Grieco, M. (2006). Raf plus TGFbeta-dependent EMT is initiated by endocytosis and lysosomal degradation of E-cadherin. Oncogene *25*, 7117–7130.

Johnson, L., Mercer, K., Greenbaum, D., Bronson, R. T., Crowley, D., Tuveson, D. A., and Jacks, T. (2001). Somatic activation of the K-ras oncogene causes early onset lung cancer in mice. Nature *410*, 1111–1116.

Jorda, M., Olmeda, D., Vinyals, A., Valero, E., Cubillo, E., Llorens, A., Cano, A., and Fabra, A. (2005). Upregulation of MMP-9 in MDCK epithelial cell line in response to expression of the Snail transcription factor. J. Cell Sci. *118*, 3371–3385.

Koenig, A., Mueller, C., Hasel, C., Adler, G., and Menke, A. (2006). Collagen type I induces disruption of E-cadherin-mediated cell-cell contacts and promotes proliferation of pancreatic carcinoma cells. Cancer Res. *66*, 4662–4671.

Lanaspa, M. A., Almeida, N. E., Andres-Hernando, A., Rivard, C. J., Capasso, J. M., and Berl, T. (2007). The tight junction protein, MUPP1, is up-regulated by hypertonicity and is important in the osmotic stress response in kidney cells. Proc. Natl. Acad. Sci. USA *104*, 13672–13677.

Li, L., Backer, J., Wong, A. S., Schwanke, E. L., Stewart, B. G., and Pasdar, M. (2003). Bcl-2 expression decreases cadherin-mediated cell-cell adhesion. J. Cell Sci. *116*, 3687–3700.

Mani, S. A. *et al.* (2008). The epithelial-mesenchymal transition generates cells with properties of stem cells. Cell *133*, 704–715.

Maretzky, T., Reiss, K., Ludwig, A., Buchholz, J., Scholz, F., Proksch, E., de Strooper, B., Hartmann, D., and Saftig, P. (2005). ADAM10 mediates E-cadherin shedding and regulates epithelial cell-cell adhesion, migration, and beta-catenin translocation. Proc. Natl. Acad. Sci. USA *102*, 9182–9187.

Oft, M., Peli, J., Rudaz, C., Schwarz, H., Beug, H., and Reichmann, E. (1996). TGF-beta1 and Ha-Ras collaborate in modulating the phenotypic plasticity and invasiveness of epithelial tumor cells. Genes Dev. *10*, 2462–2477.

Peinado, H., Olmeda, D., and Cano, A. (2007). Snail, Zeb and bHLH factors in tumour progression: an alliance against the epithelial phenotype? Nat. Rev. Cancer 7, 415–428.

Perez-Moreno, M., and Fuchs, E. (2006). Catenins: keeping cells from getting their signals crossed. Dev. Cell 11, 601–612.

Pokutta, S., and Weis, W. I. (2007). Structure and mechanism of cadherins and catenins in cell-cell contacts. Annu. Rev. Cell Dev. Biol. 23, 237–261.

Potempa, S., and Ridley, A. J. (1998). Activation of both MAP kinase and phosphatidylinositide 3-kinase by Ras is required for hepatocyte growth factor/scatter factor-induced adherens junction disassembly. Mol. Biol. Cell 9, 2185–2200.

Roberts, P. E., Phillips, D. M., and Mather, J. P. (1990). A novel epithelial cell form neonatal rat lung: isolation and differentiated phenotype. Am. J. Physiol. 259, L415–L425.

Sasaki, C. Y., Lin, H., Morin, P. J., and Longo, D. L. (2000). Truncation of the extracellular region abrogates cell contact but retains the growth-suppressive activity of E-cadherin. Cancer Res. 60, 7057–7065.

Sato, M. *et al.* (2006). Multiple oncogenic changes (K-RAS(V12), p53 knock-down, mutant EGFRs, p16 bypass, telomerase) are not sufficient to confer a full malignant phenotype on human bronchial epithelial cells. Cancer Res. 66, 2116–2128.

Sheng, H., Williams, C. S., Shao, J., Liang, P., DuBois, R. N., and Beauchamp, R. D. (1998). Induction of cyclooxygenase-2 by activated Ha-ras oncogene in Rat-1 fibroblasts and the role of mitogen-activated protein kinase pathway. J. Biol. Chem. 273, 22120–22127.

Shtutman, M., Levina, E., Ohouo, P., Baig, M., and Roninson, I. B. (2006). Cell adhesion molecule L1 disrupts E-cadherin-containing adherens junctions and increases scattering and motility of MCF7 breast carcinoma cells. Cancer Res. 66, 11370–11380.

Symowicz, J., Adley, B. P., Gleason, K. J., Johnson, J. J., Ghosh, S., Fishman, D. A., Hudson, L. G., and Stack, M. S. (2007). Engagement of collagen-binding integrins promotes matrix metalloproteinase-9-dependent E-cadherin ectodomain shedding in ovarian carcinoma cells. Cancer Res. 67, 2030–2039.

Thiery, J. P. (2002). Epithelial-mesenchymal transitions in tumour progression. Nat. Rev. Cancer 2, 442–454.

Van Putten, V., Refaat, Z., Dessev, C., Blaine, S., Wick, M., Butterfield, L., Han, S. Y., Heasley, L. E., and Nemenoff, R. A. (2001). Induction of cytosolic phospholipase A2 by oncogenic Ras is mediated through the JNK and ERK pathways in rat epithelial cells. J. Biol. Chem. 276, 1226–1232.